ACS Macro Letters

Letter

pubs.acs.org/macroletters

Self-Scrolling Nanotubular Structure of Amorphous Vinyl Polymer Containing Tetraphenylthiophene-quinoline Pendant Groups

Chung-Tin Lai and Jin-Long Hong*

Department of Materials and Optoelectronic Science, National Sun Yat-Sen University, Kaohsiung 80424, Taiwan, Republic of China

Supporting Information

ABSTRACT: In this communication, we report a scroll-like nanotubular structure found in an amorphous vinyl polymer of PS-Qu containing fluorescent tetraphenyl-quinoline (TP-Qu) pendant groups. By spin-casting dilute solution of PS-Qu, long nanoribbons with heights in correlated to the molecular width of TP-Qu pendant groups formed. On the contrast, single-, double-, and multiple-walled nanoscrolls are the major structures existing in the products from the slow-evaporation process. Presumably, scrolling of nanoribbons result in the scroll-like nanotubular structures with the resolved layer thickness in dimension close to molecular width of the TP-Qu pendant. Computer simulation on the single PS-Qu chain suggests the existence of a straight-chain backbone, with most of the vicinal 1,3-disubstituted TP-Qu groups positioned in near face-to-face arrangements. Intermolecular distances evaluated from the SAEDs were approached by the molecular dynamic of two straight-chain polymer backbones. Favorable $\pi-\pi$ interactions among the vicinal 1,3-disubstitued TP-Qu groups are suggested to be a major factor leading to the straight-chain backbone and the observed nanoribbons and nanoscrolls.

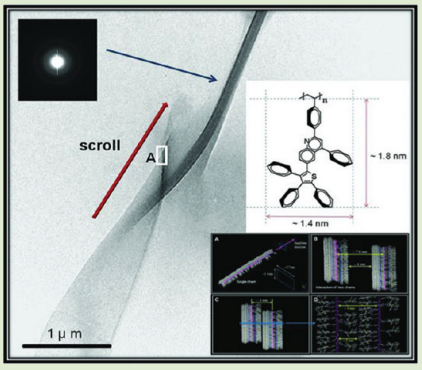

Nanotube formation from graphite by the rolling of graphene sheets is well-documented since the pioneering discovery of carbon nanotube (CNT) in 1991.[1] Thereafter, many carbon-based and inorganic compounds, such as GaN, V_2O_5, WS_2, $SrAl_2O_4$, and so on, were found to form nanotubular structures by the self-assembly and the templating techniques.[2] Comparatively fewer polymeric materials were found to form nanotubular structures despite that polymer nanotubes are particularly interesting with the hope that assemblies with large diameters and wall thickness can be constructed from.[3−7] Complex morphologies have been discovered in the fundamental forms of polymer single crystals; among them, only few examples described the scroll-like tubular structures found in the constituent lamellae of spherulites, which include form III poly(butene-1),[4] poly-(vinylvinylidene fluoride) (PVF2),[5] and poly(hexamethylene adipamide) (Nylon-6,6).[6] The potential hydrogen-bond (H-bond) interactions between the inherent amine and carbonyl groups makes Nylon-6,6 particularly interesting.[6] The H-bond interactions generate two types of folds (acid fold and amine folds) on the lamellar surface, thus, resulted in the imbalance between the inner and the outer lamellar surfaces and drove the lamellae to scroll. The imbalance of the folded basal surfaces can be turned on and off by controlling the self-seeding temperature during the crystallization stage. Besides Nylon-6,6, several recent studies on conductive polyaniline[7] also illustrated the mechanisms involved in the transformations between different self-assembled nanostructures during aqueous oxidative polymerization of aniline monomer. The nanosheet found in the beginning of the polymerization further rolled up to serve as templates for the continuous growths of different structures including nanoflakes, nanorods and nanotubes. Nanosheet and thicker structures with self-assembled layers are stabilized by H-bond and $\pi-\pi$ interactions among the aromatic rings of polyaniline. In summary, the polymeric nanoscrolls described above are all crystalline materials stabilized by the potential van der Waals, H-bond interactions, and $\pi-\pi$ stacking forces among the aromatic moieties.

In this communication, we report a scroll-like nanotubular structure from an amorphous vinyl polymer of PS-Qu[8] (Figure 1A, with M_n = 153800, M_w = 168000, and PDI = 1.09 according to GPC analysis) containing fluorescent tetraphenyl-quinoline (TP-Qu) pendant group. To the best of our knowledge, no amorphous polymer has found to self-assemble into scroll-like nanotubular structure. The polymer PS-Qu was primarily prepared to investigate its enhanced fluorescence in the aggregated solution and in the solid film states due to its novel feature of aggregation-induced emission (AIE).[9] The pendant TP-Qu group of PS-Qu was suggested to have restricted intramolecular rotation (IMR) and can be pictured as rigid board with dimension of 1.75 × 1.4 nm (Figure 1B) according to the primary simulation result. The lath-like TP-Qu pendants of PS-Qu are suggested to stiffen the main-chain, which result in the detected high T_g (at 165 °C, from DSC analysis).[8] In addition, the bulky TP-Qu pendant group is the main factor leading to the scroll nanotubular structure because of the special arrangement between the vicinal 1,3-disubstituted

Received: January 31, 2012
Accepted: March 12, 2012
Published: March 16, 2012

   dx.doi.org/10.1021/mz3000545 | ACS Macro Lett. 2012, 1, 452−456

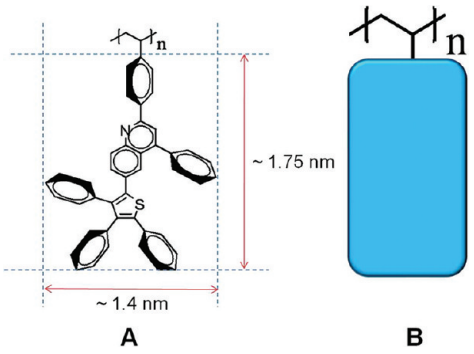

Figure 1. (A) Chemical structure of PS-Qu and (B) the lath-like pendant group of TP-Qu fluorophore.

TP-Qu pendants, which generate a near straight-chain polymer backbone, which we will discuss later in this communication.

Aomic force microscope (AFM) was preliminarily used to examine the polymer morphology observed on mica substrate. Dilute (10^{-5} M) solution of PS-Qu in THF was dropped onto a mica surface and the whole assembly was subjected to either spin-coat or slow evaporation (drop-cast) under ambient conditions to prepare specimen for AFM analysis. The AFM images suggested that the scroll nanotube is the principal structure found in the drop-cast film, in contrast to the nanoribbon structure formed in the spin-coat film. The AFM micrograph for the spin-coat sample (Figure 2A) shows the presence of long entities with randomly distributed kinked points along the contours. The assembled structures present here are very long with the lengths at least over 4 μm (most of them are longer than 10 μm) and are narrow with the widths in the ranges of 180 and 210 nm. Depth profile (Figure 2B) suggests that all the long nanoassemblies are very shallow with their heights in the ranges of 1.3 and 1.6 nm, whose values are in the vicinity of the simulated molecular width of 1.4 nm of the lath-like TP-Qu pendant depicted in Figure 1A. The large width to height ratio suggests the nanostructures discussed here are actually thin ribbons instead of tubular structures. AFM image of the drop-cast sample also shows the presence of long assemblies (Figure 2C) with the lengths extended over several micrometers. However, the long structures present here are actually more linear in shape compared to the spin-coat sample. According to the depth profiles (Figure 2D), the linear nanostructures have the heights in the ranges of 20 and 30 nm, comparatively larger than those from the spin-coat samples, which may suggest that most of them are fibers instead of ribbons and will be discussed next.

Transmission electron microscopy (TEM) was further employed to investigate the detailed morphology of PS-Qu. Specimen was prepared by the slow-evaporation of dilute solution (10^{-5} M) already deposited on the carbon-coated TEM grid. Gross inspections on the resolved TEM images suggested that besides the prevalent main structure of nanoscrolls, there are few nanoribbons distributed over the specimen. The major nanoscroll structures are presumably originated from the roll-up of the nanoribbons, which can be clearly demonstrated by the caught-up image (Figure 3) showing the progressive transformation from the bended ribbon to the scrolled tube. The particular scrolling pattern described here is in an interesting screwy path. The magnified portion (right inset) of the selected vertical edge (region A) of

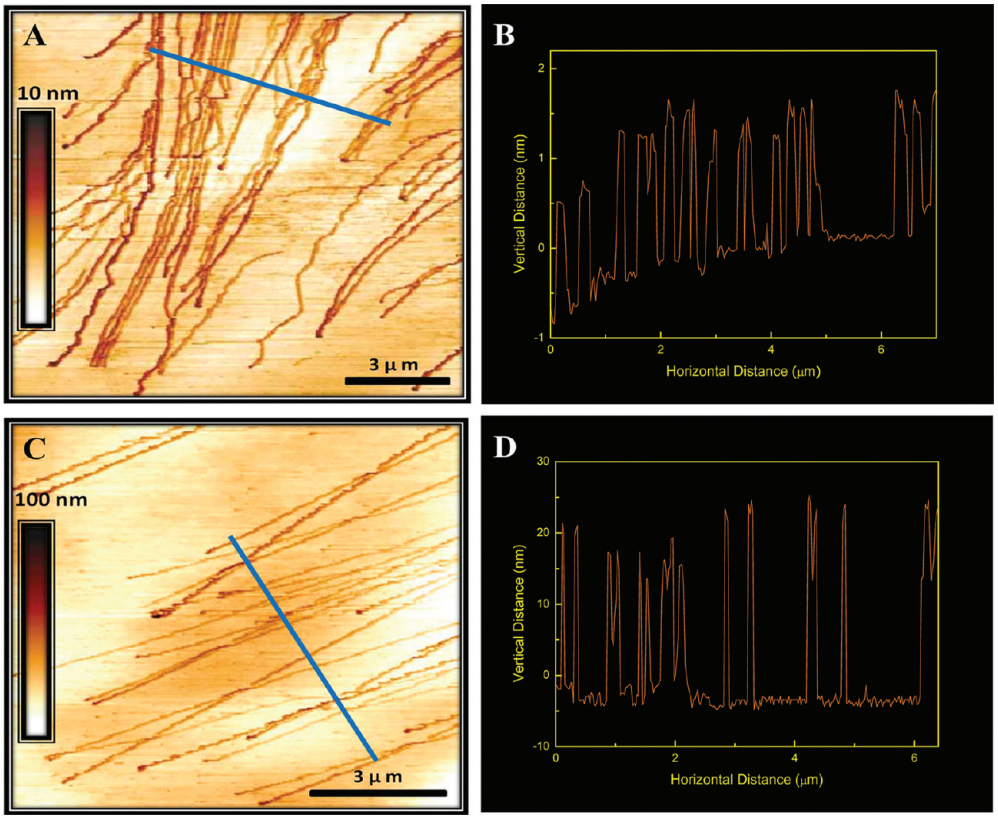

Figure 2. AFM images of PS-QU vinyl polymer from specimen prepared from (A) spin-coating and (B) slow solvent evaporation procedures; (C) and (D) are the depth profiles of the scanning lines shown in (A) and (B), respectively.

dx.doi.org/10.1021/mz3000545 | ACS Macro Lett. 2012, 1, 452−456

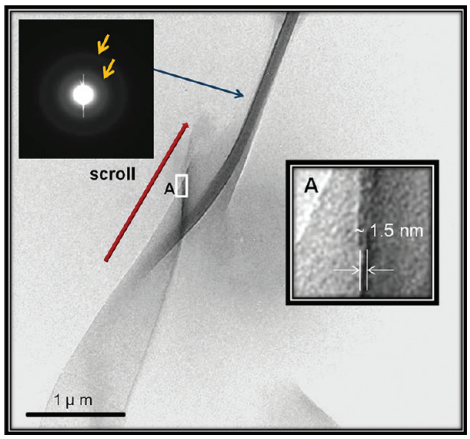

Figure 3. TEM image showing the transformation from ribbon to tubular structures (left and middle insets: SAES diffraction pattern of the selected region, right inset: magnified image of the bended area A).

the bended ribbon clearly shows that the ribbon is very thin with the layer thickness of ~1.5 nm, a value is also correlated with the heights (1.3−1.6 nm) of the nanoribbons found in the depth profile of the AFM analysis. Again, the resolved thickness (~1.5 nm) should relate to the simulated width (1.4 nm) of the lath-like TP-Qu pendant in Figure 1A. The selected area electron diffraction (SAED, left inset) consists of two diffraction halos with the corresponding *d*-spacings of 4.0 and 1.9 nm, respectively.

The scrolling of the nanoribbon should be prevalent and extensive since both the double- (Figure 4A) and the multiple-walled (Figure 4B) nanotubes were also observed in the TEM micrographs. Comparatively, the double-walled nanotube has larger dimensions than the multiple-walled tube, which may indicate that tubes with more layers come from further scrolling of the tubes with fewer layers. Here, the double-walled nanotube has an inner diameter of 130 nm and the two wall layers are separated by a distance of 10 nm (Figure 4A). The multiple-walled nanotubes (Figure 4B) have a small inner diameter of 22 nm and a close-packed wall layer with an interlayer distance of 2.5 nm. The scrolling process must be facile and extensive since at least eight layers can be resolved from the multiple-walled nanotube.

The origins of the *d*-spacings (4.0 and 1.9 nm) resolved from SAEDs (Figure 3) can be approached by theoretical simulations on the interchain distances of backbone-to-backbone and backbone-to-fluorophore. Primarily, the single-chain conformation of PS-Qu needed to be constructed. The Smart Minimizer was used to achieve the minimum-energy conformer of PS-Qu. A stereoirregular atactic conformation was used because that the starting polystyrene precursor (from anionic polymerization) synthesized for the preparation of PS-Qu is acutally atactic[8] polymer. The most favorable conformer of single-chain polymer with 100 monomer unit was created and the resulting atactic backbone after energy minimization is surprisingly straight (Figure 5A). The near face-to-face arrangements for most of the vicinal 1,3-disubsituted TP-Qu pairs is suggested to be the cause for the straight backbone. Regardless of the unfavorable bulky interaction, the $\pi-\pi$ stacking forces among the neighboring aromatic rings of the 1,3-TP-Qu groups play the decisive role leading to the final face-to-face arrangement. Separate simulations on the dimeric model compound also indicated that the face-to-face geometry is the most stable arrangement among all other possible conformers. With the constructed straight-chain backbone, the interchain distance between two energy-minimized polymer chains was then monitored and Figure 5B and C show the snapshots of the involved polymer chains pictured in the beginning and at the end of the dynamic approach process (molecular dynamics (MD) simulations), respectively. In the beginning, the polymer chains were devoid of interactions by keeping both backbones at a long distance of ~7.6 nm (Figure 5B) and then the polymer chains were manually moved toward each other until the most stable equilibrium state was finally reached, and at that point, two polymer backbones were separated by ~4 nm (Figure 5C). The magnified portion in Figure 5D illustrated the detailed chain arrangements in the equilibrium state in which regular arrays with the respective intermolecular distances of ~4 and ~2 nm are resolved, respectively. The intermolecular distances from the dynamic approach are also correlated with the *d*-spacings (4 and 1.9 nm) evaluated from the SAEDs in Figure 3. The intimate contacts among the intra- and the interchain fluorophores restrict the molecular rotations of the TP-Qu pendant groups. The densely packed fluorophores also contribute to the rigid, stiff backbone and the observed high T_g (=165 °C).

It is suggested that the interchain associations of PS-Qu occurred readily because dynamic light scatting (DLS) measurements on a dilute solution (10^{-5} M) of PS-Qu in THF revealed a large average hydrodynamic diameter over 5000 nm (Figure S-6, Supporting Information). The large polymer aggregates formed in solution should contain chain

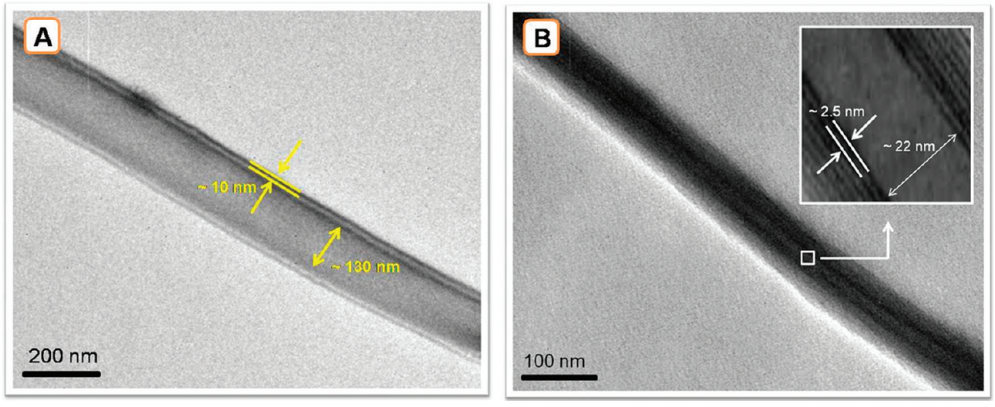

Figure 4. TEM images of (A) double- and (B) multiple-walled nanotubes.

dx.doi.org/10.1021/mz3000545 | *ACS Macro Lett.* 2012, 1, 452−456

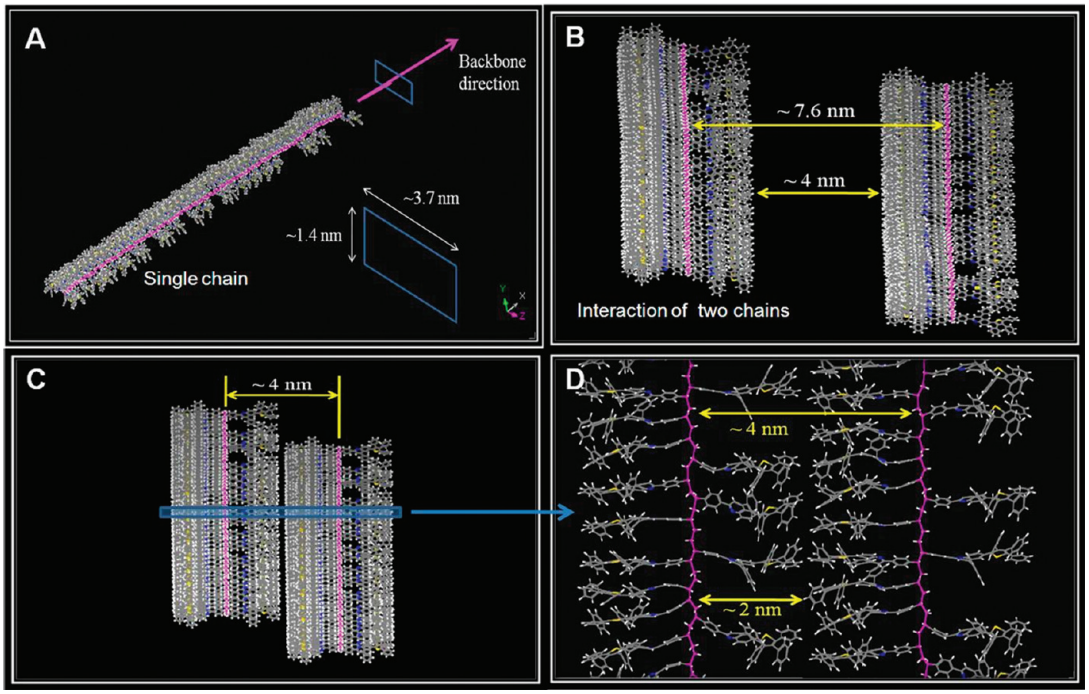

Figure 5. Simulated (A) single-chain conformation and interchain dynamics between two polymer chains in (B) the beginning and in (C) the final equilibrium state and (D) the magnified portion of the circled area in (C) showing the detailed interchain arrangement of the pendant TP-Qu groups.

segments aligning with the same direction in considering the rigid, straight-chain nature of PS-Qu and indeed, the resolved solution birefringency (Figure S-7, Supporting Information) under inspected by polarized light indicated that PS-Qu is actually a lyotropic liquid cryustalline polymer. The lyotropic solutions containing domains of oriented chains are precursors leading to the observed ribbon and scroll structures after the solvent evaporation. Further inspections by polarized optical microscope (POM) were made on the solid samples and their results suggested that substrate used in the casting process played decisive role on the final morphology. On polyethylene (PE) substrate, straight ribbons with large width (~ 20 μm, Figure S-7A, Supporting Information) and length (>500 μm) actually formed and possess unified birefringence along the whole entity. In contrast, scroll of smaller dimension (~8 μm) is the only structure observed in the sample cast on glass substrate. In this case, the scrolling structure resulted in the varied birefringence (Figure S-7B, Supporting Information) along the long chain axis. With little surface energy difference, it is reasonable to suggest that the PS-Qu chain segments tend to spread over the surface of the PE substrates to form flat ribbon structure. Instead, the large surface energy difference between the polymer PS-Qu and the glass (or mica) substrates contributed to the scrolling of the rigid, linear PS-Qu chains to reduce unfavorable contacts. Nanoscrolls (especially multiple-walled nanoscrolls) possess the geometries with limited contacts with the surface of inorganic glass substrates. Pile-up of the regular arrays of the perfectly straight chain aggregates that occurred in the solution state and during the solvent-evaporation step, in any case, should proceed rapidly in considering the facile interchain interactions of PS-Qu originated from the favorable $\pi-\pi$ stacking forces. A scrolling process was prohibited by the large centrifugal forces involved in the course of spin-coat; therefore, nanoribbons are the major structures observed in the spin-coat sample.

In summary, the nanoribbons and nanoscrolls with extended lengths over 4 μm can be prepared from spin-coat and drop-cast of dilute solutions of PS-Qu over inorganic substrates, respectively. According to AFM analysis, the height of the nanoribbons is correlated with the molecular width of the lath-like TP-Qu group. Scrolling of nanoribbons resulted in the predominant formations of single-, double-, and multiple-walled nanoscrolls with the wall thickness in a dimension close to the molecular width of the TP-Qu group, too. Computer simulation of a single PS-Qu chain resulted in a perfect straight-chain backbone with near face-to-face arrangements between the neighboring aromatic rings of the 1,3-TP-Qu groups. Molecular dynamics based on two straight-chain backbones resulted in the intermolecular distances of ~4 and ~2 nm, in correlation with the *d*-spacings (4 and 1.9 nm) evaluated from the SAEDs.

■ ASSOCIATED CONTENT

Ⓢ Supporting Information

Additional experimental detail and AFM, TEM, POM, and contact angle pictures. This material is available free of charge via the Internet at http://pubs.acs.org.

■ AUTHOR INFORMATION

Corresponding Author

*E-mail: jlhong@mail.nsysu.edu.tw. Tel.: +886-7-5252000.

Notes

The authors declare no competing financial interest.

■ ACKNOWLEDGMENTS

We appreciate the financial support from the National Science Council, Taiwan, Republic of China, under Contract No. NSC 100-2221-E-110-045.

REFERENCES

(1) Iijima, S. *Nature* **1991**, *354*, 56−58.

(2) (a) Goldberger, J.; He, R.; Zhang, Y.; Lee, S.; Yan, H.; Choi, H. J.; Yang, P. *Nature* **2003**, *422*, 599−602. (b) Ajayan, P. M.; Stephan, O.; Redlich, P.; Colliex, C. *Nature* **1995**, *375*, 564−567. (c) Hollingsworth, J. A.; Poojary, D. M.; Clearfield, A.; Buhro, W. E. *J. Am. Chem. Soc.* **2000**, *122*, 3562−3563. (d) Hacohen, Y. R.; Grunbaum, E.; Tenne, R.; Sloan, J.; Hutchison, J. L. *Nature* **1998**, *395*, 336−337. (e) Tenne, R.; Margulis, L.; Genut, M.; Hodes, G. *Nature* **1992**, *360*, 444−446. (f) Nath, M.; Rao, C. N. R. *J. Am. Chem. Soc.* **2001**, *123*, 4841−4842. (g) Feldman, Y.; Wasserman, E.; Srolovitz, D. J.; Tenne, R. *Science* **1995**, *267*, 222−225. (h) Li, Y.; Wang, J.; Deng, Z.; Wu, Y.; Sun, X.; Yu, D.; Yang, P. *J. Am. Chem. Soc.* **2001**, *123*, 9904−9905. (i) Chopra, N. G.; Luyken, R. J.; Cherrey, K.; Crespi, V. H.; Cohen, M. L.; Louie, S. G.; Zettl, A. *Science* **1995**, *269*, 966−967. (j) Ye, C.; Meng, G.; Jiang, Z.; Wang, Y.; Wang, G.; Zhang, L. *J. Am. Chem. Soc.* **2002**, *124*, 15180−15181. (k) Brorson, M.; Hansen, T. W.; Jacobsen, C. J. H. *J. Am. Chem. Soc.* **2002**, *124*, 11582−11583. (l) Hong, S. Y.; Popovitz-Biro, R.; Prior, Y.; Tenne, R. *J. Am. Chem. Soc.* **2003**, *125*, 10470−10474. (m) Gautam, U. K.; Vivekchand, S. R. C.; Govindaraj, A.; Kulkarni, G. U.; Selvi, N. R.; Rao, C. N. R. *J. Am. Chem. Soc.* **2005**, *127*, 3658−3659. (n) Ye, C.; Bando, Y.; Shen, G.; Golberg, D. *Angew. Chem., Int. Ed.* **2006**, *45*, 4922−4926. (o) Nath, M.; Rao, C. N. R. *Angew. Chem., Int. Ed.* **2002**, *41*, 3451−3454. (p) Chen, J.; Tao, Z.; Li, S. *Angew. Chem., Int. Ed.* **2003**, *42*, 2147−2151. (q) Hacohen, Y. R.; Popovitz-Biro, R.; Grunbaum, E.; Prior, Y.; Tenne, R. *Adv. Mater.* **2002**, *14*, 1075−1078. (r) Chen, J.; Tao, Z.; Li, S.; Fan, X.; Chou, S. *Adv. Mater.* **2003**, *15*, 1379−1382.

(3) Steinhart, M.; Wendorff, J. H.; Greiner, A.; Wehrspohn, R. B.; Nielsch, K.; Schilling, J.; Choi, J.; Gosele, U. *Science* **2002**, *296*, 1997−1997.

(4) Holland, V. F.; Miller, R. L. *J. Appl. Phys.* **1964**, *35*, 3241−3248.

(5) Vaughan, A. S. *J. Mater. Sci.* **1993**, *28*, 1805−1813.

(6) Cai, W.; Li, C. Y.; Li, L.; Lotz, B.; Keating, M.; Marks, D. *Adv. Mater.* **2004**, *16*, 600−605.

(7) (a) Huang, J.; Kaner, R. B. *J. Am. Chem. Soc.* **2004**, *126*, 851−855. (b) Zujovic, Z. D.; Laslau, C.; Bowmaker, G. A.; Kilmartin, P. A.; Webber, A. L.; Brown, S. P.; Sejdic, J. T. *Macromolecules* **2010**, *43*, 662−670. (c) Zhang, L.; Wan, M. *Nanotechnology* **2002**, *13*, 750−755. (d) Laslau, C.; Zujovic, Z. D.; Sejdic, J. T. *Macromol. Rapid Commun.* **2009**, *30*, 1663−1668. (e) Zhang, L.; Wan, M. *Adv. Funct. Mater.* **2003**, *13*, 815−820. (f) Zhang, L.; Long, Y.; Chen, Z.; Wan, M. *Adv. Funct. Mater.* **2004**, *14*, 693−698. (g) Huang, Y. F.; Lin, C. W. *Polymer* **2009**, *50*, 775−782. (h) Laslau, C.; Zujovic, Z.; Travas-Sejdic, J. *Prog. Polym. Sci.* **2010**, *35*, 1403−1419. (i) Zujovic, Z.; Laslau, C.; Travas-Sejdic, J. *Chem. Asian J.* **2011**, *6*, 791−796.

(8) Lai, C. T.; Hong, J. L. *J. Phys. Chem. B* **2010**, *114*, 10302−10310.

(9) (a) Xie, J. Z.; Lam, J. W. Y.; Cheng, L.; Chen, H.; Qiu, C.; Kwok, H. S.; Zhan, X.; Liu, Y.; Zhu, D.; Tang, B. Z. *Chem. Commun.* **2001**, 1740−1741. (b) Hong, Y.; Lama, J. W. Y.; Tang, B. Z. *Chem. Commun.* **2009**, 4332−4353. (c) Liu, J.; Lam, J. W. Y.; Tang, B. Z. *J. Inorg. Organomet. Polym.* **2009**, *19*, 249−285.